General and Comparative Endocrinology 362 (2025) 114675

Contents lists available at ScienceDirect

General and Comparative Endocrinology

journal homepage: www.elsevier.com/locate/ygcen

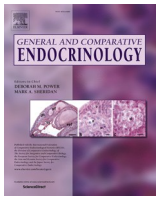

Research paper

Effect of blocking transforming growth factor-β/Activin-Myostatin signaling on the expression of ecdysteroid metabolism and responsive genes in the crustacean molting gland (Y-organ)

Samiha A.M. Benrabaa [a], Donald L. Mykles [a,b,*]

[a] Colorado State University, Fort Collins, CO 80523, USA
[b] Bodega Marine Laboratory, University of California, Davis, Bodega Bay, CA 94923, USA

ARTICLE INFO

Keywords:
TGFβ/Activin signaling
Ecdysteroid
Y-organ
Molting
Halloween gene
Myostatin

ABSTRACT

Molting in decapod crustaceans is controlled by ecdysteroids synthesized and secreted by the molting gland, or Y-organ (YO). The YO undergoes phenotypic changes in ecdysteroid production that drive molt cycle stage transitions; these are the basal, activated, committed, and repressed states in the intermolt, early premolt, mid- and late premolt, and postmolt stages, respectively. Reduced secretion of molt-inhibiting hormone (MIH) by a neurosecretory center in the eyestalk ganglia activates the YO and the animal transitions to early premolt. During premolt, transforming growth factor-beta (TGFβ)/Activin-Myostatin (Mstn) signaling mediates the transition of the YO from the activated to the committed state, as SB431542 blocks this transition. In the blackback land crab, *Gecarcinus lateralis*, the YO expresses genes involved in ecdysteroid synthesis (*Gl-NADK*, *Gl-ALAS* and Halloween genes *Gl-Nvd*, *Gl-Spo*, *Gl-Phm*, *Gl-Dib*, and *Gl-Sad*) and catabolism (*Gl-CYP18a1*); ecdysteroid signaling (ecdysteroid responsive genes *Gl-EcR*, *Gl-RXR*, *Gl-Br-C*, *Gl-HR3*, *Gl-HR4*, *Gl-E74*, *Gl-E75*, and *Gl-Ftz-f1*); and *Gl-FOXO*. Intermolt adult *G. lateralis* were induced to molt by eyestalk ablation (ESA) and injected with either dimethyl sulfoxide (DMSO) vehicle (control) or SB431542 in DMSO (experimental) at Day 0. ESA increased hemolymph ecdysteroid titer at 1, 3, and 5 days post-ESA in both control and experimental groups, indicating that SB431542 had no effect on YO activation. Ecdysteroid titer did not increase further in the experimental group at 7 and 14 days post-ESA, indicating that SB431542 prevented transition of the YO to the committed state. ESA with or without SB431542 had no effect on the mRNA levels of the eight ecdysteroid metabolism genes, seven of the eight ecdysteroid responsive genes (the only exception was *Gl-E74* at 1 day post-ESA), and *Gl-FOXO* at 1, 3, and 5 days post-ESA. Compared to the control group, SB431542 lowered the mRNA level of *Gl-Nvd* at 7 and 14 days post-ESA and mRNA levels of *Gl-Spo*, *Gl-Phm*, *Gl-Dib*, *Gl-Sad, Gl-CYP18a1, Gl-ALAS*, *Gl-NADK, Gl-EcR*, *Gl-RXR*, *Gl-Br-C*, and *Gl-FOXO* at 14 days post-ESA. SB431542 had no effect on the mRNA levels of *Gl-HR3 Gl-HR4, Gl-E74, Gl-E75* and *Gl-Ftz-f1*. These results suggest that TGFβ/Activin-Mstn signaling maintains the mRNA levels of genes needed for increased ecdysteroid synthesis and signaling in the committed YO during mid- and late premolt.

1. Introduction

Decapod crustaceans must molt to grow, as shedding of the old skeleton and expansion of a new skeleton at ecdysis creates an enlarged internal space for tissue growth (Mykles, 2024). Molting is controlled by two endocrine organs: the X-organ/sinus gland (XO/SG) complex in the eyestalk ganglia and the molting glands, or Y-organs (YOs) in the anterior cephalothorax (Mykles, 2024; Skinner, 1985). The YOs synthesize and secrete ecdysteroid hormones, which initiate and coordinate processes during the premolt stage, such as degradation and absorption of the inner layers of the old exoskeleton, synthesis of the new exoskeleton, growth of limb regenerates, and atrophy of the claw muscle; these processes are essential for successful ecdysis (Mykles, 2024). Ecdysteroid biosynthesis is catalyzed by *Neverland* (*Nvd*) dehydrogenase and cytochrome p450 (CYP) enzymes encoded by the Halloween genes *Spook* (*Spo*), *Phantom* (*Phm*), *Disembodied* (*Dib*), *Shadow* (*Sad*), and *Shade* (*Shd*) in insects or *Shed* in crustaceans (Mykles, 2011; Mykles and Chang, 2020; Swall et al., 2021). *Shd* and *Shed* encode 20-hydroxylases that convert inactive precursors (e.g., ecdysone) to active hormones (e.g., 20-hydroxyecdysone or 20E) (Mykles, 2011; Swall et al., 2021). NAD kinase

* Corresponding author at: Colorado State University, Fort Collins, CO 80523, USA.
E-mail address: donald.mykles@colostate.edu (D.L. Mykles).

https://doi.org/10.1016/j.ygcen.2025.114675
Received 4 July 2024; Received in revised form 4 February 2025; Accepted 5 February 2025
Available online 7 February 2025

(NADK) and 5-aminolevulinic acid synthase (ALAS) are necessary for ecdysteroid synthesis in insects (Nakaoka et al., 2017). A 26-hydroxylase, encoded by *Cyp18a1*, inactivates ecdysteroids (Mykles, 2011).

The YOs are negatively regulated by molt-inhibiting hormone (MIH), a neuropeptide secreted by the XO/SG complex. MIH binds to high-affinity receptors on the YO membrane, activating cyclic nucleotide-dependent inhibition of ecdysteroid synthesis (Mykles, 2021, 2024). Consequently, entry into premolt is triggered by a reduction in MIH release from the XO/SG complex, which activates the YOs (Mykles and Chang, 2020). Molting can be experimentally induced in many species, including the blackback land crab (*Gecarcinus lateralis*), by eyestalk ablation (ESA), as the eyestalk ganglia are the major source of MIH (Mykles and Chang, 2020; Skinner, 1985). Molting can also be induced by multiple limb autotomy (MLA; Mykles, 2024; Skinner, 1985).

The molt cycle is unidirectional and consists of four main stages: intermolt, premolt, ecdysis, and postmolt. Phenotypic changes in the YO are associated with transitions between stages and determine the sequential progression through the molt cycle, as one transition leads to the next. In *G. lateralis*, these YO phenotypes are the basal, activated, committed, and repressed states, which occur during intermolt (stage C_4), early premolt (stage D_0), mid- and late premolt (stages D_1 and $D_{2\text{-}3}$), and postmolt (stages A, B, and $C_{1\text{-}3}$), respectively (Mykles, 2024; Mykles and Chang, 2020). Pulsatile release of MIH from the XO/SG complex maintains the YO in the basal state, which has low ecdysteroid secretion rates. A reduction in MIH triggers the transition from the basal state to the activated state in early premolt. This transition requires mechanistic Target of Rapamycin Complex 1 (mTORC1) activity, as rapamycin prevents YO activation (Abuhagr et al., 2014b, 2016; Shyamal et al., 2018). In *G. lateralis*, YO activation relies primarily on mTORC1-dependent translation of transcripts needed for ecdysteroid synthesis, as the mRNA levels of Halloween genes *Gl-Nvd*, *Gl-Spo*, *Gl-Phm*, *Gl-Dib*, and *Gl-Sad* are not increased in early premolt (Benrabaa et al., 2023). The activated YO remains sensitive to MIH and other factors, so that premolt can be suspended when environmental conditions become unfavorable, or by the loss of a limb regenerate (Mykles, 2024; Skinner, 1985). The YO may also be regulated by growth factors, as it expresses tyrosine kinase receptors for insulin-like peptide (ILP), epidermal growth factor, fibroblast growth factor, and platelet-derived/vascular endothelial growth factor (Flores et al., 2024; Mykles, 2021). A downstream target of insulin/ILP signaling is FOXO, a transcription factor that controls mTORC1-dependent ecdysteroid synthesis in the insect prothoracic gland (Benrabaa et al., 2024; Kannangara et al., 2021).

A critical decision point is reached at the end of early premolt, when the animal becomes committed to molt in mid-premolt and begins synthesis of the new exoskeleton (Mykles, 2021, 2024). Transition of the YO from the activated to committed state requires Transforming Growth Factor-beta (TGFβ)/Activin-Myostatin (Mstn) signaling, as SB431542 prevents this transition without affecting YO activation (Abuhagr et al., 2016). Moreover, rapamycin delays animals from entering mid-premolt, indicating that the YO must first be activated before it can transition to the committed state (Abuhagr et al., 2016). The committed YO becomes insensitive to MIH due to the down-regulation of MIH signaling genes, which assures that premolt processes proceed without interruption (Das et al., 2018). High ecdysteroidogenic activity by the committed YO is associated with up-regulation of mTORC1 signaling genes (Das et al., 2018), Halloween genes *Gl-Sad* and *Gl-Shed5A*, ecdysteroid responsive gene *Gl-HR3*, and *Gl-FOXO* (Benrabaa et al., 2023, 2024; Swall et al., 2021). The increased expression of *Gl-FOXO* and *Gl-HR3* during premolt suggests that insulin-dependent and ecdysteroid-dependent signaling, respectively, are involved in the transcriptional up-regulation of *Gl-mTOR* (Abuhagr et al., 2016; Benrabaa et al., 2024). The transition of the YO from the committed to repressed state occurs at the end of late premolt and coincides with the peak in hemolymph ecdysteroid titer (Mykles, 2021; Mykles and Chang, 2020). The ecdysteroidogenic activity of the repressed YO is low, which results in a hemolymph ecdysteroid titer that is lower than the titers in the other molt stages (Mykles, 2011). The mRNA levels of many signaling genes, including those in the MIH, mTOR, and TGFβ/Activin-Mstn pathways, are at their lowest, suggesting that the repressed YO is removed from normal hormonal control until the YO transitions back to the basal state at the end of postmolt (Das et al., 2018; Mykles, 2021).

The *G. lateralis* YO expresses genes encoding ecdysteroid metabolism enzymes (*Gl-Nvd*, *Gl-Spo*, *Gl-Phm*, *Gl-Dib*, *Gl-Sad*, *Gl-Shed*, and *Gl-Cyp18a1)*, ecdysteroid responsive nuclear receptors (*Gl-EcR*, *Gl-RXR*, *Gl-BrC*, *Gl-E74*, *Gl-E75*, *Gl-HR3*, *Gl-HR4*, and *Gl-Ftz-f1*), and *Gl-FOXO* (Benrabaa et al., 2023, 2024; Swall et al., 2021). ESA does not increase the mRNA levels of these genes at 1 day and 3 days post-ESA, indicating that YO activation depends on increased mTORC1-dependent translation (Benrabaa et al., 2023, 2024; Swall et al., 2021). Here we report the effects of blocking TGFβ/Activin-Mstn-dependent YO commitment on the expression of these same genes by quantitative polymerase chain reaction (qPCR). *G. lateralis* were eyestalk-ablated and injected with either SB431542 (experimental group) or vehicle alone (control group). YOs were harvested from intact animals (Day 0) and from ESA animals at one to 14 days post-ESA. A Day 5 time point was included, as this is the time point at which the YO transitions to the committed state at Day 7 post-ESA (Abuhagr et al., 2016). The results indicate that TGFβ/Activin-Mstn signaling up-regulates or sustains the expression of ecdysteroid metabolism and responsive genes in mid- and late premolt.

2. Materials and methods

2.1. Animals and experimental treatment

Adult male *Gecarcinus lateralis* were shipped from the Dominican Republic and maintained at Colorado State University, CO at ~ 27 °C, ~80 % relative humidity, and a 12 h/12 h light/dark cycle (Covi et al., 2010). Communal cages contained aspen bedding moistened with 5 ppt Instant Ocean (Aquarium Systems, Mentor, OH) and changed once per week. Crabs were fed lettuce, carrots, and raisins twice a week. Animals were acclimated at least one month before experimental treatment.

Eyestalk ablation (ESA) was used to experimentally induce molting (Skinner, 1985). On Day 0, intermolt animals were eyestalk-ablated and received a single injection of either SB431542 (Selleck Chemicals, Houston, TX) in dimethyl sulfoxide (DMSO) or DMSO alone (control) delivered through the arthrodial membrane at the base of a walking leg. To achieve estimated final concentrations of 10 μM SB431542 and 0.1 % DMSO in the hemolymph, the following equation was used to calculate the volumes to inject: total body weight (g) x 0.3 μl 10 mM SB431542 stock or DMSO, assuming a hemolymph volume of 30 % of wet weight (Abuhagr et al., 2016). Hemolymph and YOs were harvested at Days 0 (intact animals), 1, 3, 5, 7, and 14 post-ESA. YOs were placed in 350 μl RNAlater (Ambion) overnight at 4 °C and then stored at 20 °C. Hemolymph samples (100 μl) were combined immediately with 300 μl methanol and centrifuged for 10 min at 20,000 xg at 4 °C to precipitate denatured protein. 20-Hydroxyecdysone (20E) in supernatants was quantified with a competitive ELISA using a 1:64 K dilution of 20E-horseradish peroxidase conjugate and a 1:100 K dilution of rabbit anti-20E antibody as described (Abuhagr et al., 2014a; Kingan, 1989). The commercial reagents used in the ELISA were AffiniPure Goat Anti-Rabbit Fc fragment-specific secondary antibody from Jackson ImmunoResearch (catalog #111–005-008) and the SeraCare TMB Peroxidase Kit. Data are presented as mean ± 1 S.E.M. pg 20E equivalents/μl hemolymph (n = number of biological replicates).

2.2. Y-organ gene expression

Total RNA was isolated using a Trizol and chloroform-phenol procedure as described in (Covi et al., 2010). Briefly, RNA pellets from the first chloroform-phenol extraction were dissolved in 22 μl RNase/DNase/protease-free water. DNase I (Thermo Fisher Scientific, Grand Island, NY) treatment followed the manufacturer's instructions.

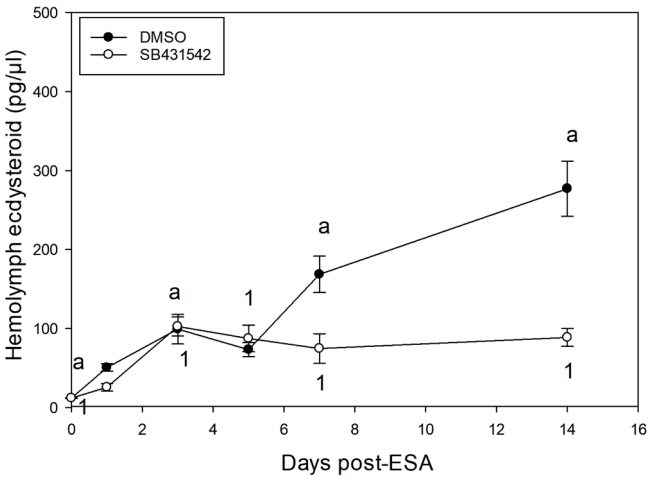

Fig. 1. Effect of SB431542 on hemolymph ecdysteroid titer in *G. lateralis*. Intermolt male adults were eyestalk-ablated and received a single injection of either 10 mM SB431542 in DMSO (~10 µM and ~ 0.1 % final hemolymph concentrations, respectively) or DMSO (~0.1 % final hemolymph concentration) at Day 0. Data are presented as mean ± 1 S.E.M. pg 20E equivalents/µl hemolymph (n = 8 for Day 0 and 1; n = 7 for Days 3, 5, and 7; n = 6 for Day 14). Those means within the control group that were significantly different from Day 0 are indicated by the same letter. Those means within the experimental group that were significantly different from Day 0 are indicated by the same number. Asterisks indicate means in the experimental group that were significantly different from the means in the control group at the same time point.

Ribolock (10 units; Thermo Fisher Scientific) was included in the DNase I treatment to prevent RNA degradation. The RNA solution was subjected to a second phenol–chloroform extraction and RNA was precipitated by adding 0.5 vol 3 M sodium acetate (pH 5.2) to 1.5 vol of isopropanol. The pellets were dissolved in 22 µl RNase/DNase/protease free water and RNA concentrations were quantified with a NanoDrop 1000 Spectrophotometer (Thermo Fisher). cDNA was synthesized in reactions containing 4 µl RNA and SuperScript IV Reverse Transcriptase (Thermo Fisher) in accordance with the manufacturer's instructions (Abuhagr et al., 2016). cDNA samples were stored at −15 °C.

Quantitative polymerase chain reaction (qPCR) was performed using a LightCycler 480 Thermocycler (Roche Applied Science, Indianapolis, IN, USA). The primers were the same as those used in (Benrabaa et al., 2023, 2024). The GenBank accession numbers are: *Gl-NADK* (OP722285), *Gl-ALAS* (OP572284), *Gl-Nvd* (OP555905), *Gl-Spo* (OP555906) *Gl-Phm* (OP555907), *Gl-Dib* (OP555908), *Gl-Sad* (OP555909), *Gl-CYP18a1* (OP555910), *Gl-EcR* (OQ915377), *Gl-RXRa* (DQ067280), *Gl-Br-C* (OQ915378), *Gl-HR3* (OR037290), *Gl-HR4* (OQ985202), *Gl-E74* (OQ970168), *Gl-E75* (DQ058409), *Gl-Ftz-f1* (OQ995023), and *Gl-FOXO* (OR021934). Reactions contained 0.5 µl each of forward and reverse gene-specific primers, 5 µl SYBR Green Master Mix (Roche Applied Science), 3 µl nuclease free water, and 1 µl cDNA template. The PCR conditions were an initial denaturation at 95 °C for 3 min; 45 cycles at 95 °C for 30 sec, 62 °C for 30 sec, and 72 °C for 20 sec; and a final extension time of 7 min at 72 °C. Standard curves of serial dilutions of PCR products were used to calculate mRNA copy number (Benrabaa et al., 2023, 2024). Data are presented as mean $\log_{10}$ copy number per µg total RNA ± 1 S.E.M. (n = number of biological replicates).

2.3. Statistical analyses and software

SigmaPlot 12.0 (Systat 27 Software, San Jose, CA USA) was used for statistical analysis and graphing. ANOVA and Tukey post-hoc tests were used to determine statistical significance between groups ($p < 0.05$). A Dunn's post-hoc test was used if equal variance tests failed ($p < 0.05$).

3. Results

ESA resulted in an increase on hemolymph ecdysteroid titer by three days post-ESA in both control and experimental animals (Fig. 1). There was no significant difference between the means of control and experimental animals at 1, 3, and 5 day(s) post-ESA, indicating that SB431542 had no effect on YO activation and entry into early premolt. However, SB431542 prevented the increases in hemolymph ecdysteroid titer that occurred in control animals at 7 and 14 days post-ESA, indicating that the experimental treatment blocked YO commitment and the transition to mid-premolt (Fig. 1).

The expression of the eight ecdysteroid metabolism genes in the YO showed similar patterns between control and experimental animals. ESA ± SB431542 had no significant effect on mRNA levels of all eight genes in intact (Day 0) and at 1, 3, and 5 day(s) post-ESA (Fig. 2). In control animals, ESA had no significant effect at 1, 3, and 5 days post-ESA for *Gl-Nvd* (Fig. 2A) or at 1, 3, 5, and 7 days post-ESA for *Gl-Spo*, *Gl-Phm*, *Gl-Dib*, *Gl-Sad*, *Gl-CYP18a1*, *Gl-ALAS*, and *Gl-NADK* (Fig. 2B-H, respectively). The *Gl-Nvd* mRNA level at 7 and 14 days post-ESA was higher than that at Day 0 (Fig. 2A). For the other seven genes, the mRNA levels at 14 days post-ESA were higher than those at Day 0 (Fig. 2B-H). SB431542 had a delayed effect on gene expression. The mRNA levels in the experimental group were significantly lower than those in the control group at 7 and 14 days post-ESA for *Gl-Nvd* (Fig. 2A) and at 14 days post-ESA for *Gl-Spo*, *Gl-Phm*, *Gl-Dib*, *Gl-Sad*, *Gl-CYP18a1*, *Gl-ALAS*, and *Gl-NADK* (Fig. 2B-H, respectively).

ESA ± SB431542 had mostly no effect on the mRNA levels of the eight ecdysteroid responsive genes and *Gl-FOXO* at 1, 3, 5, and 7 days post-ESA (Fig. 3). In the control group, the mRNA levels of *Gl-EcR*, *Gl-RXR*, *Gl-Br-C*, *Gl-E74*, and *Gl-HR4* at 14 days post-ESA were significantly higher than those at Day 0 (Fig. 3A, B, C, E, and G, respectively). The mRNA level of *Gl-E74* at 1 day post-ESA was also significantly higher (Fig. 3E). In the experimental group, the mRNA levels of *Gl-EcR*, *Gl-RXR*, *Gl-Br-C*, and *Gl-FOXO* at 14 days post-ESA were significantly lower than those in the control group (Fig. 3A, B, C, and I, respectively). By contrast, SB431542 had no effect on the mRNA levels of *Gl-E75*, *Gl-E74*, *Gl-HR3*, *Gl-HR4*, and *Gl-Ftz-f1* (Fig. 3D, E, F, G, and H, respectively).

4. Discussion

The *G. lateralis* YO undergoes critical phase transitions over the molt cycle. The first major transition occurs from intermolt to early premolt, when environmental and physiological conditions are suitable to initiate molting. This transition is mediated by the MIH signaling pathway, which consists of cAMP-dependent triggering and cGMP-dependent summation phases that are linked by Ca^{2+}/calmodulin/NO synthase (Mykles and Chang, 2020). It is hypothesized that a cGMP-dependent protein kinase inhibits mTORC1 activity, which maintains the YO in the basal state (Mykles, 2021). This explains the apparent contradiction that the basal YO has a low ecdysteroid synthetic rate, even though the mRNA levels of the Halloween genes are high at this stage, and do not increase in early premolt in MLA animals or at 1 and 3 days post-ESA (Benrabaa et al., 2023). In other words, YO ecdysteroid synthesis during intermolt and early premolt is not correlated with the mRNA levels of Halloween genes. Rather, it is driven by mTORC1-dependent global translation of mRNAs to proteins (Mykles, 2021). Thus, the basal YO is effectively primed to respond rapidly to a drop in MIH release, as indicated by increasing hemolymph ecdysteroid titer by 1 day post-ESA (Fig. 1) (Abuhagr et al., 2016; Benrabaa et al., 2023; Covi et al., 2010).

mTORC1 activity is also necessary for YO commitment, as rapamycin delays this transition and affects, either directly or indirectly, the expression of thousands of genes (Abuhagr et al., 2016; Shyamal et al., 2018). YO commitment requires mTORC1-dependent gene expression, including the up-regulation of mTOR signaling genes in mid- and late premolt (Abuhagr et al., 2014b; Wittmann et al., 2018). One target is TGFβ/Activin-Mstn signaling, which regulates gene expression by Smad

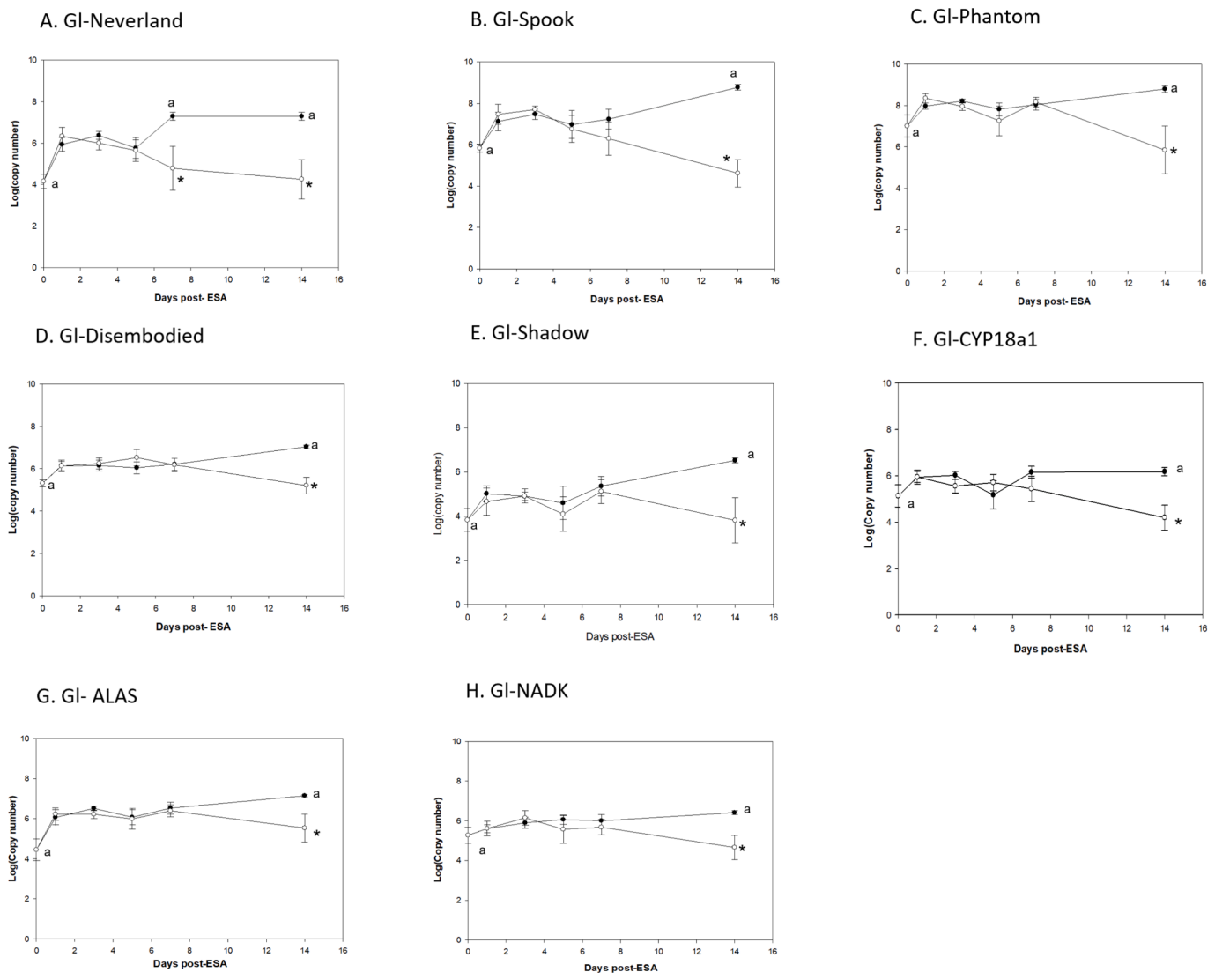

Fig. 2. Effects of SB431542 on expression of ecdysteroid metabolism genes in *G. lateralis* YO. YOs were harvested from the control (●) and experimental (○) animals in Fig. 1 and mRNA levels were quantified by qPCR. Data are presented as mean ± 1 S.E.M. $\log_{10}$ copy number/μg total RNA. Those means within the control group that were significantly different from Day 0 are indicated by the same letter. Asterisks indicate means in the experimental group that were significantly different from the means in the control group at the same time point.

transcription factors (Aashaq et al., 2021; Du et al., 2024; Truman and Riddiford, 2023). A Mstn-like Activin factor is highly expressed in crustacean YO and muscle (Abuhagr et al., 2016; Covi et al., 2008; Musgrove et al., 2024). Mstn is secreted to the extracellular matrix as a latent complex, which is proteolytically activated by extracelluar metalloproteinases (Suh and Lee, 2020). *Gl-Mstn* expression is increased in the activated YO and peaks in early premolt in MLA animals and at Day 3 in ESA animals (Abuhagr et al., 2016; Das et al., 2018; Shyamal et al., 2018).

SB431542 was used to determine the effects of blocking YO commitment without affecting YO activation on gene expression. Previous studies showed that the mRNA levels of eight ecdysteroid metabolism genes did not increase in activated YOs from animals induced to molt by either ESA or MLA (Benrabaa et al., 2023, 2024). These results were confirmed and extended in this study, as the mRNA levels were the same between control and experimental groups at 1, 3, and 5 day(s) post-ESA and were not significantly different from the mRNA levels in intact animals at Day 0 (Fig. 2). At 5 days post-ESA, the YO transitions from the activated state at 3 days post-ESA to the committed state at 7 days post-ESA (Abuhagr et al., 2016; Covi et al., 2010). It is notable that the hemolymph titers between the control and experimental groups did not diverge until at 7 and 14 days post-ESA (Fig. 1), which indicates that the YOs in the control group had transitioned to the committed state, while the YOs in the experimental group did not. SB431542 had similar effects on the expression for seven of the eight ecdysteroid metabolism genes at 7 and 14 days post-ESA, with the means in the experimental group significantly lower than those in the control group at Day 14 (Fig. 2B-H). *Gl-Nvd* was expressed at significantly lower levels at Days 7 and 14 (Fig. 2A). Nvd catalyzes the first reaction in the ecdysteroid biosynthetic pathway, converting cholesterol to 7-dehydrocholesterol (Mykles, 2011). The differences were mostly due to higher mRNA levels in the control group relative to those at Day 0, as the means in the experimental group were not significantly different from those at Day 0 (Fig. 2). These data suggest that sustained or increased expression of ecdysteroid metabolism genes contributes to increased ecdysteroid synthesis and secretion by the committed YO.

The *G. lateralis* YO expresses ecdysteroid receptor (*Gl-EcR/Gl-RXR*) and six other ecdysteroid responsive genes. This suggests that the YO responds to increased hemolymph 20E titers during premolt. Binding of 20E to EcR/RXR initiates a transcriptional cascade of nuclear hormone

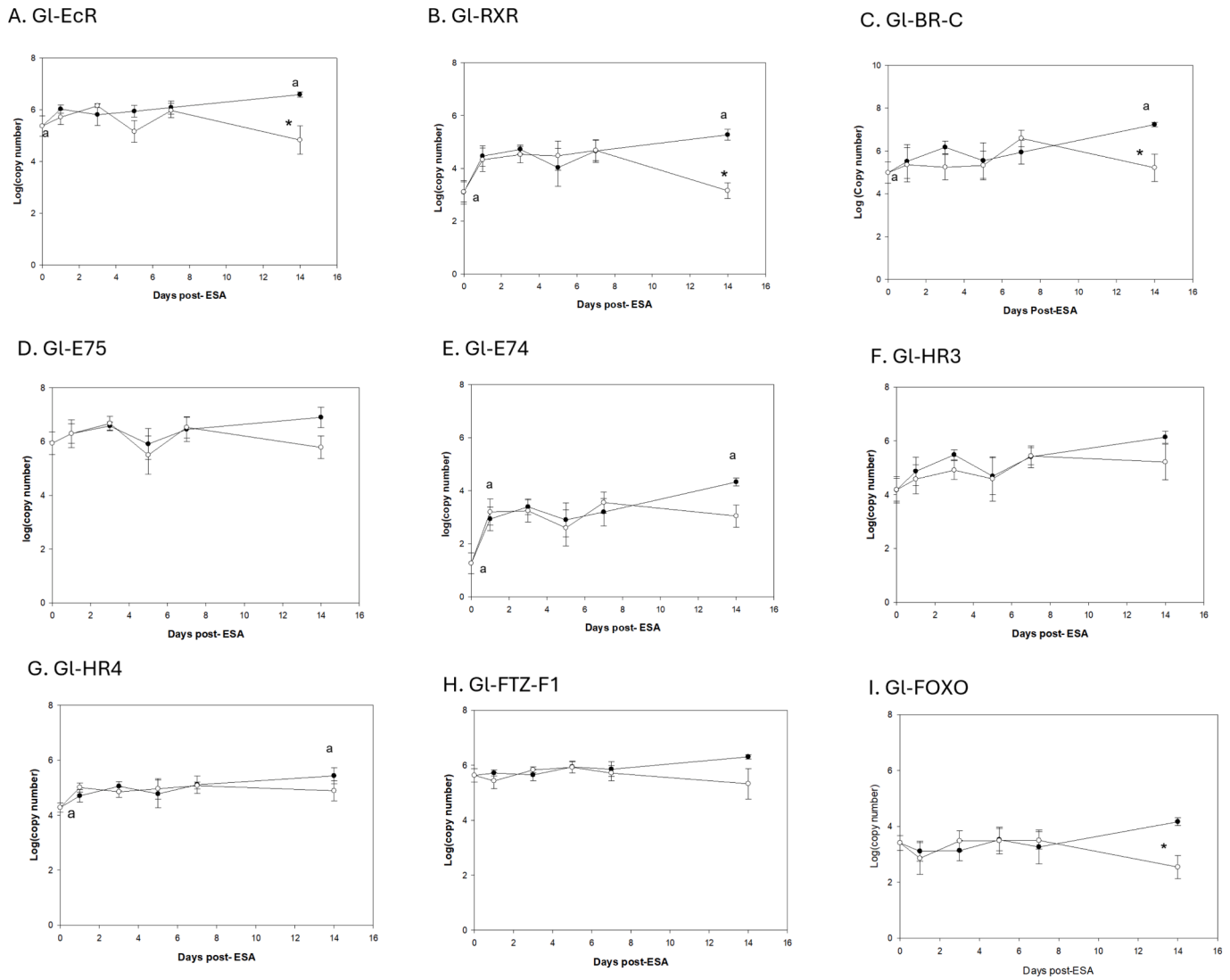

Fig. 3. Effects of SB431542 on expression of ecdysteroid responsive and FOXO genes in *G. lateralis* YO. YOs were harvested from the control (●) and experimental (○) animals in Fig. 1 and mRNA levels were quantified by qPCR. Data are presented as mean ± 1 S.E.M. $\log_{10}$ copy number/μg total RNA. Those means within the control group that were significantly different from Day 0 are indicated by the same letter. Asterisks indicate means in the experimental group that were significantly different from the means in the control group at the same time point.

receptors that up-regulate expression of Halloween genes (Knigge et al., 2021). *Gl-HR3* mRNA level is increased at mid- and late premolt in MLA animals, which is correlated with increased expression of Halloween genes *Gl-Sad* and *Gl-Shed5A* (Benrabaa et al., 2023, 2024; Swall et al., 2021). However, in ESA animals, the mRNA levels of the eight ecdysteroid responsive genes are not correlated with hemolymph ecdysteroid titer (Benrabaa et al., 2024). ESA with or without SB431542 had no effect on the mRNA levels of the eight ecdysteroid responsive genes at 1, 3, 5, and 7 days(s) post-ESA (Fig. 3A-H). Unlike the ecdysteroid metabolism genes (Fig. 2), SB431542 had no consistent effect on gene expression. The only difference between the control and experimental groups was at Day 14. SB431542 lowered the mRNA levels of *Gl-EcR*, *Gl-RXR*, and *Gl-Br-C* (Fig. 3A, B, and C), but had no effect on the mRNA levels of the other five genes (Fig. 3D-H).

FOXO is a Forkhead box O class transcription factor that links ILP signaling with mTORC1 activity in the insect prothoracic gland (Kannangara et al., 2021). MLA increases *Gl-FOXO* expression during premolt and postmolt stages (Benrabaa et al., 2024), suggesting that the YO is more sensitive to ILPs at these molt stages (Mykles, 2021). By contrast, ESA had no effect on *Gl-FOXO* expression in control animals (Fig. 3I) (Benrabaa et al., 2024). SB431542 lowered *Gl-FOXO* mRNA level at Day 14 post-ESA (Fig. 3I). These data suggest that the committed YO maintains *Gl-FOXO* mRNA level.

The effects of ESA and MLA on gene expression in the committed YO could not be more striking. MLA is considered a physiologically relevant method to induce molting, as animals often lose limbs to predation or injury and must molt to restore a functional appendage; in *G. lateralis*, loss of five or more walking legs stimulates molting (Liu et al., 2024; Mykles, 2024; Skinner, 1985). Animals do not enter premolt immediately. Instead, *G. lateralis* enter premolt 4 to 6 weeks post-MLA (Mykles, 2024). ESA induces molting by an acute withdrawal of MIH, which results in immediate YO activation (Fig. 1) (Abuhagr et al., 2016; Benrabaa et al., 2023; Covi et al., 2010). Although ESA serves as a useful experimental tool to synchronize premolt processes, ESA may disrupt other physiological processes, such as carbohydrate and lipid metabolism, reproduction, and ion and water balance, that are coordinated by other neuropeptides produced in the XO/SG complex (Fehsenfeld, 2024; Webster, 2015). Eyestalk-ablated *G. lateralis* proceed through premolt, but fail to molt successfully (Mykles, 2024). In MLA animals, the mRNA levels of Halloween genes *Gl-Sad* and *Gl-Shed-5A*, ecdysteroid responsive gene *Gl-HR3*, and *Gl-FOXO* increase in the committed YO (Abuhagr et al., 2014b; Benrabaa et al., 2023, 2024; Swall et al., 2021).

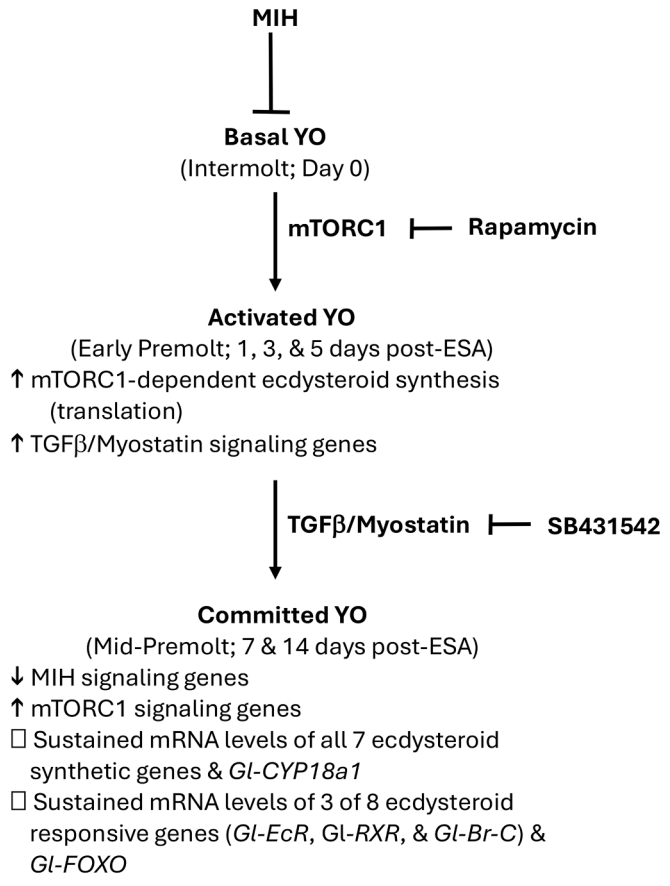

Fig. 4. Summary diagram of the effects of eyestalk ablation (ESA) ± SB5431542 on gene expression in the *G. lateralis* Y-organ. During intermolt, molt-inhibiting hormone (MIH) maintains the YO in the basal state by inhibiting mechanistic Target of Rapamycin Complex 1 (mTORC)1-dependent translation of ecdysteroid synthesis genes. ESA activates YO ecdysteroidogenesis and the animal enters early premolt by 1 day post-ESA. The basal to activated transition is blocked by the mTORC1 inhibitor rapamycin. Upregulation of TGFβ/Activin-Myostatin (Mstn) signaling genes in the activated YO by 5 days post-ESA drives the transition of the YO to the committed state and entry into mid-premolt at 7 days post-ESA. SB431542, an inhibitor of TGFβ/Activin-Mstn signaling, blocks this transition. The committed YO downregulates MIH signaling genes and upregulates mTORC1 signaling genes. mRNA levels of 7 ecdysteroid synthesis, *Gl-CYP18a1*, *Gl-EcR*, *Gl-RXR*, and *Gl-FOXO* genes were sustained or elevated in the committed YO, as SB431542 lowered mRNA levels of the 11 genes by 14 days post-ESA. Data from this study and Benrabaa et al. (2023, 2024) and Shyamal et al. (2018); reviewed in Mykles (2021).

By contrast, ESA had comparatively little, if any, effect on the mRNA levels of ecdysteroid metabolism and ecdysteroid responsive genes in the committed YO at 7 and 14 days post-ESA (Figs. 2 and 3), even though the YO increases ecdysteroid synthesis and secretion, as indicated by increased hemolymph ecdysteroid titer (Fig. 1) (Abuhagr et al., 2016; Benrabaa et al., 2023, 2024; Covi et al., 2010; Swall et al., 2021). ESA up-regulates mTORC1 signaling genes, which are inhibited by rapamycin (Abuhagr et al., 2016; Shyamal et al., 2018). These data suggest that the YO in ESA animals increases mTORC1 activity to sustain high ecdysteroid synthetic rates (Fig. 4).

5. Conclusions

YO ecdysteroid synthesis involves both transcriptional and post-translational regulation of mTORC1 and TGFβ/Activin-Mstn signaling in *G. lateralis* induced to molt by MLA or ESA. First, increased YO ecdysteroidogenesis in early premolt requires mTORC1-dependent global translation of mRNAs into proteins (Mykles and Chang, 2020). YO activation does not require increased expression of Halloween genes, *Gl-ALAS*, and *Gl-NADK* (Fig. 2) (Benrabaa et al., 2023). In other words, the mRNA levels of biosynthetic genes in the basal YO are sufficient to increase the ecdysteroid synthetic capacity of the activated YO, enabling the YO to respond rapidly to the drop in MIH circulating in the hemolymph. Second, TGFβ/Activin-Mstn signaling drives the transition to the committed state, as SB431542 prevents or delays this transition (Fig. 1) (Abuhagr et al., 2016). In MLA *G. lateralis*, YO commitment is associated with transcriptional up-regulation of mTORC1 signaling, ecdysteroid metabolism, ecdysteroid responsive, and *Gl-FOXO* genes, which coincides with increased ecdysteroid synthesis and secretion in mid- and late premolt (Abuhagr et al., 2016; Benrabaa et al., 2023, 2024; Das et al., 2018; Swall et al., 2021). However, ESA uncoupled ecdysteroid metabolism and responsive gene expression from ecdysteroid synthesis (Figs. 2 and 3) (Benrabaa et al., 2024; Swall et al., 2021). This suggests that there is greater a reliance on mTORC1 activity for the increase in hemolymph ecdysteroid titer in mid- and late premolt in eyestalk-ablated animals.

CRediT authorship contribution statement

Samiha A.M. Benrabaa: Writing – review & editing, Writing – original draft, Visualization, Methodology, Investigation, Formal analysis, Data curation, Conceptualization. **Donald L. Mykles:** Writing – review & editing, Writing – original draft, Supervision, Project administration, Funding acquisition, Conceptualization.

Declaration of Competing Interest

The authors declare that they have no known competing financial interests or personal relationships that could have appeared to influence the work reported in this paper.

Acknowledgements

This research was supported by grants from the National Science Foundation (IOS-1257732 and IOS-1922701). We thank Hector C. Horta and Rafael Polanco for collecting *G. lateralis* and the Ministry of Environment and Natural Resources of the Dominican Republic under Contract for Access to Genetic Resources for Research Purposes DJC-1-2019-01310 and Collection and Export Permit No. VAPS-07979.

Data availability

Data will be made available on request.

References

Aashaq, S., Batool, A., Mir, S.A., Beigh, M.A., Andrabi, K.I., Shah, Z.A., 2021. TGF-beta signaling: a recap of SMAD-independent and SMAD-dependent pathways. J. Cell. Physiol. 327, 59–85.

Abuhagr, A.M., Blindert, J.L., Nimitkul, S., Zander, I.A., LaBere, S.M., Chang, S.A., MacLea, K.S., Chang, E.S., Mykles, D.L., 2014a. Molt regulation in green and red color morphs of the crab *Carcinus maenas*: gene expression of molt-inhibiting hormone signaling components. J. Exp. Biol. 217, 796–808.

Abuhagr, A.M., MacLea, K.S., Chang, E.S., Mykles, D.L., 2014b. Mechanistic target of rapamycin (mTOR) signaling genes in decapod crustaceans: Cloning and tissue expression of mTOR, Akt, Rheb, and p70 S6 kinase in the green crab, *Carcinus maenas*, and blackback land crab, *Gecarcinus lateralis*. Comp. Biochem. Physiol. 168A, 25–39.

Abuhagr, A.M., MacLea, K.S., Mudron, M.R., Chang, S.A., Chang, E.S., Mykles, D.L., 2016. Roles of mechanistic target of rapamycin and transforming growth factor-beta signaling in the molting gland (Y-organ) of the blackback land crab, *Gecarcinus lateralis*. Comp. Biochem. Physiol. 198A, 15–21.

Benrabaa, S.A.M., Chang, S.A., Chang, E.S., Mykles, D.L., 2023. Effects of molting on the expression of ecdysteroid biosynthesis genes in the Y-organ of the blackback land crab. *Gecarcinus lateralis*. Gen. Comp. Endocrinol. 340, 114304.

Benrabaa, S.A.M., Chang, S.A., Chang, E.S., Mykles, D.L., 2024. Effects of molting on the expression of ecdysteroid responsive genes in the crustacean molting gland (Y-organ). Gen. Comp. Endocrinol. 355, 114548.

Covi, J.A., Bader, B.D., Chang, E.S., Mykles, D.L., 2010. Molt cycle regulation of protein synthesis in skeletal muscle of the blackback land crab, *Gecarcinus lateralis*, and the differential expression of a myostatin-like factor during atrophy induced by molting or unweighting. J. Exp. Biol. 213, 172–183.

Covi, J.A., Kim, H.W., Mykles, D.L., 2008. Expression of alternatively spliced transcripts for a myostatin-like protein in the blackback land crab, *Gecarcinus lateralis*. Comp. Biochem. Physiol. 150A, 423–430.

Das, S., Vraspir, L., Zhou, W., Durica, D.S., Mykles, D.L., 2018. Transcriptomic analysis of differentially expressed genes in the molting gland (Y-organ) of the blackback land crab, *Gecarcinus lateralis*, during molt-cycle stage transitions. Comp. Biochem. Physiol. 28D, 37–53.

Du, R.C., Wen, L.Q., Niu, M., Zhao, L.T., Guan, X.Y., Yang, J., Zhang, C.M., Liu, H.L., 2024. Activin receptors in human cancer: Functions, mechanisms, and potential clinical applications. Biochem. Pharmacol. 222, 116061.

Fehsenfeld, S., 2024. Endocrinology. In: Weihrauch, D., McGaw, I.J. (Eds.), Ecophysiology of the European Green Crab (*Carcinus maenas)* and Related Species: Mechanisms behind the Success of a Global Invader. Academic Press, London, pp. 159–178.

Flores, K.A., Pérez-Moreno, J.L., Durica, D.S., Mykles, D.L., 2024. Phylogenetic and transcriptomic characterization of insulin and growth factor receptor tyrosine kinases in crustaceans. Front. Endocrinol. 15, 1379231.

Kannangara, J.R., Mirth, C.K., Warr, C.G., 2021. Regulation of ecdysone production in *Drosophila* by neuropeptides and peptide hormones. Open Biology 11, 200373.

Kingan, T.G., 1989. A competitive enzyme-linked immunosorbent assay - Applications in the assay of peptides, steroids, and cyclic nucleotides. Anal. Biochem. 183, 283–289.

Knigge, T., LeBlanc, G.A., Ford, A.T., 2021. A crab is not a fish: Unique aspects of the crustacean endocrine system and considerations for endocrine toxicology. Front. Endocrinol. 12, 587608.

Liu, L., Tao, D., Wang, C., Fu, Y., Wang, S., Huang, X., Zhai, W., Song, W., 2024. Autotomy and regeneration of appendages in crustaceans: a review. J. Ocean Univ. China 23, 731–742.

Musgrove, L., Russell, F.D., Ventura, T., 2024. Considerations for cultivated crustacean meat: potential cell sources, potential differentiation and immortalization strategies, and lessons from crustacean and other animal models. Crit. Rev. Food Sci. Nutr. 2024, 2342480.

Mykles, D.L., 2011. Ecdysteroid metabolism in crustaceans. J. Steroid Biochem. Molec. Biol. 127, 196–203.

Mykles, D.L., 2021. Signaling pathways that regulate the crustacean molting gland. Front. Endocrinol. 12, 674711.

Mykles, D.L., 2024. Molting physiology, in: S. Saleuddin, S.P. Leys, R.D. Roer, I. Wilkie (Eds.), Frontiers in Invertebrate Physiology, Vol. 2: Crustacea. Apple Academic Press, Palm Bay, FL, 229-274.

Mykles, D.L., Chang, E.S., 2020. Hormonal control of the crustacean molting gland: Insights from transcriptomics and proteomics. Gen. Comp. Endocrinol. 294, 113493.

Nakaoka, T., Iga, M., Yamada, T., Koujima, I., Takeshima, M., Zhou, X.Y., Suzuki, Y., Ogihara, M.H., Kataoka, H., 2017. Deep sequencing of the prothoracic gland transcriptome reveals new players in insect ecdysteroidogenesis. PloS One 12, e0172951.

Shyamal, S., Das, S., Guruacharya, A., Mykles, D.L., Durica, D.S., 2018. Transcriptomic analysis of crustacean molting gland (Y-organ) regulation via the mTOR signaling pathway. Sci. Rep. 8, 7307.

Skinner, D.M., 1985. Molting and regeneration. In: Bliss, D.E., Mantel, L.H. (Eds.), The Biology of Crustacea. Academic Press, New York, pp. 43–146.

Suh, J., Lee, Y.S., 2020. Similar sequences but dissimilar biological functions of GDF11 and myostatin. Exp. Molec. Med. 52, 1673–1693.

Swall, M.E., Benrabaa, S.A.M., Tran, N.M., Tran, T.D., Ventura, T., Mykles, D.L., 2021. Characterization of *Shed* genes encoding ecdysone 20-monooxygenase (CYP314A1) in the Y-organ of the blackback land crab. *Gecarcinus lateralis*. Gen. Comp. Endocrinol. 301, 113658.

Truman, J.W., Riddiford, L.M., 2023. *Drosophila* postembryonic nervous system development: a model for the endocrine control of development. Genetics 2023, 1–31.

Webster, S.G., 2015. Endocrinology of metabolism and water balance: Crustacean hyperglycemic hormone. In: Chang, E.S., Thiel, M. (Eds.), The Natural History of the Crustacea: Physiology. Oxford Press, Oxford, pp. 36–67.

Wittmann, A.C., Benrabaa, S.A.M., Lopez-Ceron, D.A., Chang, E.S., Mykles, D.L., 2018. Effects of temperature on survival, moulting, and expression of neuropeptide and mTOR signalling genes in juvenile Dungeness crab (*Metacarcinus magister*). J. Exp. Biol. 221, jeb187492.